Bioorganic & Medicinal Chemistry Letters 26 (2016) 1803–1808

Contents lists available at ScienceDirect

Bioorganic & Medicinal Chemistry Letters

journal homepage: www.elsevier.com/locate/bmcl

Structure-based design and development of (benz)imidazole pyridones as JAK1-selective kinase inhibitors

Vladimir Simov [a,*], Sujal V. Deshmukh [c], Christopher J. Dinsmore [b], Fiona Elwood [a], Rafael B. Fernandez [a], Yudith Garcia [a], Craig Gibeau [a], Hakan Gunaydin [a], Joon Jung [d], Jason D. Katz [a], Brian Kraybill [e], Blair Lapointe [a], Sangita B. Patel [a], Tony Siu [a], Hua Su [a], Jonathan R. Young [f]

[a] Merck & Co., 33 Avenue Louis Pasteur, Boston, MA, United States
[b] FORMA Therapeutics, 500 Arsenal Street #100, Watertown, MA, United States
[c] Novartis Institutes for BioMedical Research, Inc., 250 Massachusetts Avenue, Cambridge, MA, United States
[d] Ironwood Pharmaceuticals, 301 Binney Street, Cambridge, MA, United States
[e] Alcon Laboratories, 6201 South Freeway, Fort Worth, TX, United States
[f] Celgene Corporation, 4550 Towne Centre Court, San Diego, CA, United States

ARTICLE INFO

Article history:
Received 21 January 2016
Revised 11 February 2016
Accepted 13 February 2016
Available online 19 February 2016

Keywords:
Janus Kinase
JAK1 kinase inhibitor
Structure-based design

ABSTRACT

The mammalian Janus Kinases (JAK1, JAK2, JAK3 and TYK2) are intracellular, non-receptor tyrosine kinases whose activities have been associated in the literature and the clinic with a variety of hyperproliferative diseases and immunological disorders. At the onset of the program, it was hypothesized that a JAK1 selective compound over JAK2 could lead to an improved therapeutic index relative to marketed non-selective JAK inhibitors by avoiding the clinical AEs, such as anemia, presumably associated with JAK2 inhibition.

During the course of the JAK1 program, a number of diverse chemical scaffolds were identified from both uHTS campaigns and *de novo* scaffold design. As part of this effort, a (benz)imidazole scaffold evolved via a scaffold-hopping exercise from a mature chemical series. Concurrent crystallography-driven exploration of the ribose pocket and the solvent front led to analogs with optimized kinome and JAK1 selectivities over the JAK2 isoform by targeting several residues unique to JAK1, such as Arg-879 and Glu-966.

The mammalian Janus Kinases (JAK1, JAK2, JAK3 and TYK2) are intracellular, non-receptor tyrosine kinases involved in the signal transduction of pro-inflammatory cytokine receptors.[1] Association of the JAK proteins with cytokine receptors in various heterodimers, trimers and homodimers leads to JAK activation, followed by phosphorylation of STAT proteins and gene transcription, thereby driving diverse cellular processes.[2] Currently marketed pan-selective JAK inhibitors have shown clinical success in the treatment of myelofibrosis and rheumatoid arthritis,[3] albeit the clinical efficacy has been dose-limited by hematopoietic adverse events likely driven through the non-selective inhibition of JAK2 and the erythropoietin (EPO) signaling pathway.[4] At the onset of the program, it was hypothesized that a superior therapeutic window could be achieved by selectively targeting the JAK1 pathway, specifically by measuring inhibition of IL-6, while avoiding the limiting blood-related adverse events by sparing the JAK2 EPO pathway.[5]

During the course of the Merck JAK1 program, several structurally diverse chemical scaffolds were identified from both an uHTS campaign and *de novo* scaffold design. A promising new structural class of pyrazole carboxamides emerged from this approach (**1** in Fig. 1), which was subsequently optimized for drug-like properties and JAK1 selectivity.[6] Concurrently, an effort to identify additional structural matter, such as a chemical series with different properties and improved JAK1 selectivity, was initiated by employing a scaffold-hopping strategy from pyrazole carboxamide **1**, as shown in Figure 1. As part of this approach, a structurally diverse pyridone benzimidazole scaffold was designed by applying three structural modifications, including (1) carboxamide cyclization to reveal the pyridone moiety, (2) ring-opening of the pyrazole and (3) cyclization to arrive at the solvent-front benzimidazole ring.[7] By maintaining the carboxamide 2-point HBD/HBA hinge interaction in **1**, as well as the 4-aminopyran ribose pocket moiety, the early objective was to conserve the

* Corresponding author. Tel.: +1 617 992 3267.
E-mail address: vladimir_simov@merck.com (V. Simov).

http://dx.doi.org/10.1016/j.bmcl.2016.02.035
0960-894X/

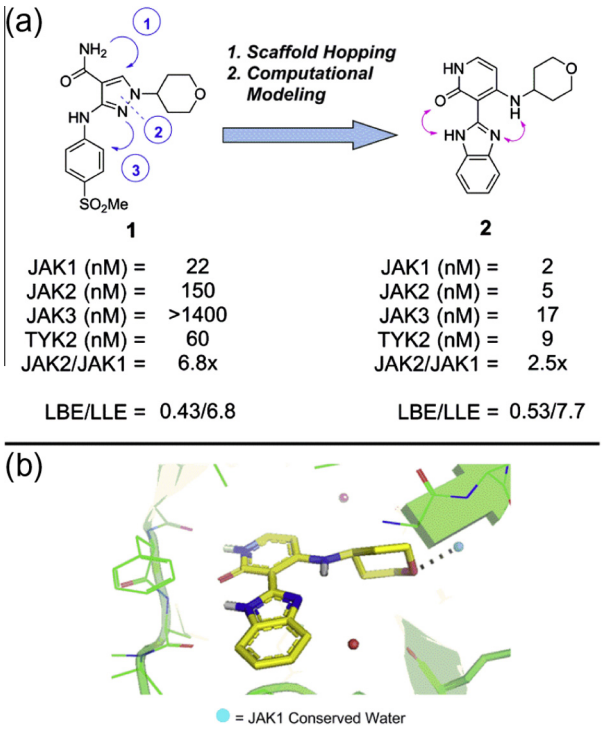

Figure 1. (a) Scaffold hopping strategy leading to benzimidazole pyridone lead compound **2**; (b) in yellow, docking of **2** in JAK1 crystal structure.

Table 1
In vitro JAK enzyme activity

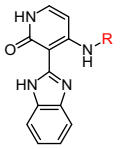

Entry	R	JAK1 (nM)	JAK2/1 ratio	LBE	LLE
3	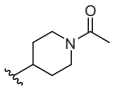	10	1.6	0.43	7.1
4	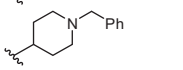	5	2.6	0.39	5.4
5	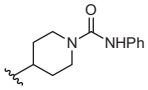	5	2.1	0.36	6.3
6		1.6	3.3	0.54	7.8
7		26	3.2	0.46	6.5
8	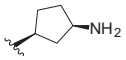	3.2	10	0.52	7.8
9	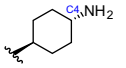	0.6	6.7	0.54	8.0
10	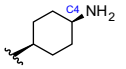	0.1	40	0.58	8.8

favorable JAK1 potency and promising selectivity observed with the benchmark compound **1**. As shown in Figure 1, pyridone benzimidazole **2** exhibited 10-fold improvement in JAK1 potency relative to its precursor **1**, as well as excellent ligand efficiencies, albeit the isoform selectivity was diminished. Therefore, the early focus of the medicinal chemistry effort shifted toward an improvement of the JAK1 selectivity, especially over the JAK2 isoform.

The initial approach at achieving the targeted levels of JAK1 selectivity (JAK2/JAK1 > 15-fold) and potency (JAK1 IC_{50} < 10 nM) in the enzymatic assay was heavily based on computational modeling.[8] In particular, the early strategy relied on targeting a conserved water molecule observed near the P-loop of the ribose pocket in several of the internal JAK1 crystal structures (Fig. 1b). It was hypothesized that JAK1 selectivity may be achieved by directly engaging this crystallographic water with larger ribose pocket substituents via either (a) H-bonding interaction (*ex.* pyran **2** in Fig. 1b, and piperidine **6** in Table 1) or (b) water displacement (*ex.* acetamide **3**, *trans*-1,4-cyclohexyl diamine **9**, as well as the corresponding *trans*-1,4-cyclohexyl aminoalcohol and aminonitrile analogs, not shown). Simultaneously, by increasing the size of the ribose pocket substitution toward the P-loop water molecule, we hoped to gain an additional JAK1 selectivity over JAK2 by taking advantage of a more flexible and accommodating JAK1 P-loop relative to a less dynamic region found in JAK2 (cf. **4** and **5**, Table 1).[9] To that end, a range of cycloalkyl ribose pocket groups were prepared projecting a variety of substitutions toward this conserved water molecule, including substituted azetidines, pyrrolidines and piperidines. Subsequently, a variety of acyclic P-loop amines were also explored (vide infra). This approach quickly yielded several potent piperidine JAK1 inhibitors, although no notable improvement in the JAK2/JAK1 isoform selectivity was observed relative to the benchmark pyrazole **1** (**2**–**5**, Fig. 1b and Table 1).

Although disappointed by the lack of isoform selectivity improvement observed with the initial P-loop SAR, we were intrigued by the excellent ligand efficiencies (LBE = 0.54 and LLE = 7.8) and modest improvement in both JAK1 potency and selectivity observed with the unsubstituted piperidine **6**. Expanding on the basic free amine SAR was initially unsuccessful, as the isomeric piperidines (e.g., **7**) and related heterocycloalkyl amines (e.g., pyrrolidines and azetidine; not shown) exhibited diminished potencies and JAK1 selectivities. Pleasingly, moving the basic amine out of the cycloalkyl ring, as shown with the *cis*-cyclopentyl 1,3-diamine **8**, restored the JAK1 potency with a notable improvement in isoform selectivity (10-fold). Subsequent optimization of the exocyclic amine led to *cis*-1,4-cyclohexyl diamine **10**, which not only exhibited excellent JAK1 potency (IC_{50} = 0.1 nM) and ligand efficiencies (LBE = 0.58, LLE = 8.8), but also a 40-fold JAK2/JAK1 selectivity in the primary enzymatic assays. Interestingly, the corresponding *trans*-isomer **9** showed significantly diminished isoform selectivity relative to **10**, suggesting that the C4 cyclohexyl amine indeed forms distinct interactions with JAK1 compared to the JAK2 protein.

To gain further insight into the unique role of the exocyclic amine with respect to the JAK1 potency and selectivity, a crystal structure of **10** bound to the JAK1 protein was obtained (Fig. 2). As expected, the pyridone hinge binder is involved in a 2-point HBD/HBA interaction with the JAK1 protein, including: (1) a hydrogen bond with the JAK1 Leu-939 amide NH and (2) a hydrogen bond with the JAK1 Glu-957 carbonyl moiety. In addition, a unique and unexpected binding mode of the ribose pocket cyclohexyl diamine was apparent. The cyclohexyl amine did not project toward the P-loop region, as originally hypothesized in Figure 1, but rather adopted a unique conformation to orient the C4 amine toward the solvent front. This unexpected binding mode was a result of the pyridone occupying an axial cyclohexyl orientation to enable the formation of three distinct hydrogen bond interactions between the C4 amine and (1) the hydroxyl side-chain of Ser-963, (2) the Glu-966 carboxylate, both of which are water-mediated (2.7 Å), as well as (3) a direct hydrogen bond with the backbone carbonyl

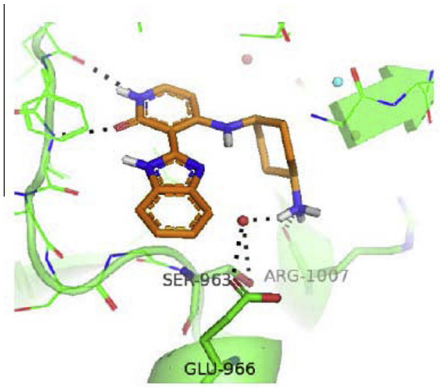

Figure 2. X-ray structure of **10** (orange) in JAK1 (green) highlighting the three key H-bond interactions with Ser-963, Glu-966 and Arg-1007 (RCSB PDB code: 5HX8).

of Arg-1007 (2.9 Å). Although initially surprised by the axial orientation of the pyridone, according to quantum mechanical calculations the cyclohexyl bioactive conformation observed in the crystal structure represents the lowest energy conformer by 0.8 kcal/mol.[10]

Comparison of the JAK family amino acid homology in proximity to the C4 amine, in particular focusing on the three aforementioned JAK1 residues, revealed a potential source of the 40-fold JAK1 selectivity. While both JAK1 and JAK2 contain analogous Ser and Arg residues (i.e., Ser-963 vs Ser-935 and Arg-1007 vs Arg-980, respectively), a difference exists between the Glu-966 residue in JAK1 and the analogous Asp-939 found in JAK2. It is hypothesized that the shorter aspartic acid side-chain forms a less optimal water-mediated H-bond with the C4 amine of **10** relative to the glutamic acid found in JAK1, therefore accounting for the improved JAK1 potency and thus isoform selectivity.[11] Hence, we believe that this particular interaction is key for the observed JAK1 selectivity in **10** and can be further utilized to build in additional isoform selectivity over JAK2.

With this information in hand, a new endeavor was initiated to explore the SAR of the C4 amine substitution, both in terms of the amine sterics and electronics. While a number of small alkyl and acyl substituents (not shown) were well tolerated with respect to their JAK1 potency, a strong correlation between the basicity of the amine and the JAK2/JAK1 isoform selectivity emerged (see **11**–**15**, Table 2). In particular, a decrease in isoform selectivity correlated well with a decrease in calculated amine basicity. Ultimately it was determined that pK_a values >9 were necessary to achieve the targeted levels of isoform selectivity (>15-fold).[8] Interestingly, modulating the basicity of the amine did not have a significant impact on the JAK1 potency, but only affected the JAK2 binding. It is hypothesized that the higher dissolvation penalty to form a water-mediated H-bond between a more basic amine and Glu-966 in JAK1 can be off-set by the ideal geometry of this water network interaction, whereas the less ideal geometry in JAK2 is more sensitive to changes in the amine pK_a and therefore the dissolvation penalty.

In addition to the good in vitro stability (HLM Cl_{int} <15 mL min^{-1} kg^{-1} and HHep Cl_{int} = 12 mL min^{-1} kg^{-1}), compound **10** proved to be a valuable tool compound to interrogate the JAK1 biology in an in vitro setting (Table 3). The JAK1 cell-based activity of **10**, as measured by IL-6 cytokine inhibition in a pathway reporter gene assay, was measured at 3 nM with an EPO/IL-6 pathway selectivity of 16-fold.[12] In addition, **10** exhibited excellent activity in both a PBMC (peripheral blood mononuclear cell) functional assay measuring IL-7/STAT5 inhibition and the corresponding rat whole blood variant.[13] Furthermore, the pathway selectivity and functional activity of **10** compared favorably to the two marketed JAK inhibitors, tofacitinib and ruxolitinib, as predicted by their enzyme potency profile.

With the JAK1 isoform selectivity SAR well established, the broad kinome panel selectivity of the representative pyridone benzimidazole **10** was evaluated against other non-JAK kinases.[14] Compound **10** was tested against 265 kinases and exhibited >100-fold selectivity relative to JAK1 for 97% of the measured kinases (Table 4). While the overall kinome selectivity profile was promising, the FLT3 inhibitory off-target activity of **10** was of particular interest. FLT3 signaling is important for RA pathogenesis by playing an essential role in the in vivo differentiation of dendritic cells and could therefore interfere with the interpretation of the JAK1-driven biology with our tool compound, therefore prompting us to explore strategies to avoid FLT3 inhibition.[15]

Based on available crystallographic information, overlay between the FLT3 and JAK1 ATP-binding pockets suggested several residue differences that could potentially be exploited to circumvent the FLT3 off-target activity. The first strategy was designed to take advantage of the rigidity of the FLT3 phenylalanine

Table 2
Correlation between JAK1 potency, isoform selectivity and basicity of C4 amine

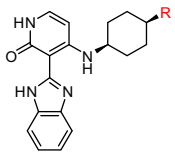

Entry	R	ACD pK_a	JAK1 (nM)	JAK2/1 ratio
11		10.5	0.3	26
12	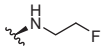	8.8	0.5	5.4
13	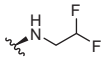	6.6	0.7	2.5
14	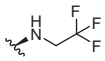	4.8	2	1.3
15	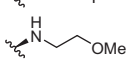	9.2	0.8	19

Table 3
In vitro JAK enzyme and cell (reporter and functional) activities for **10** compared to tofacitinib and ruxolitinib

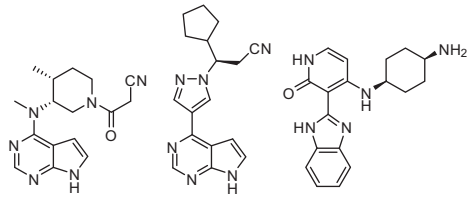

	Tofacitinib	Ruxolitinib	**10**
Enzymatic assay			
JAK1 IC_{50} (nM)	1.3	0.43	0.1
JAK2 IC_{50} (nM; JAK2/1 ratio)	1.4 (1×)	0.12 (0.3×)	4.0 (40×)
JAK3 IC_{50} (nM)	0.35	2.8	2.5
TYK2 IC_{50} (nM)	12.8	0.72	1.5
Reporter cell assay			
JAK1 (IL-6, nM)	95	40	3
JAK2 (EPO, nM)	71	8	48
Functional assay			
PBMC (IL-7/STAT5, nM)	39	448	17
Rat WB (IL-7/STAT5, nM)	139	na	40

Table 4
In vitro enzyme selectivity of **10** over other non-JAK kinases ($N = 265$ kinases measured at Invitrogen)

Enzymatic IC_{50}	Kinase off-target IC_{50}	JAK1-fold selectivity
JAK1 = 0.1 nM	NUAK1 = 2 nM	20×
	BRSK1 = 2 nM	20×
	SNF1LK2 = 4 nM	40×
	FLT3 = 5 nM	50×
	AMPKa1 = 5.5 nM	55×
	PDGFRA = 9 nM	90×

gatekeeper residue Phe-691, rather than the more flexible and accommodating Met-956 residue found in JAK1, by introducing a variety of substitutions at the pyridone C3 position (R^1 in Fig. 3). While this approach did show initial promise with respect to the JAK1 potency ($IC_{50} = 2$ nM for $R_1 = CN$ analog of **10**, not shown), the C3 pyridone SAR had a detrimental effect on the overall kinome selectivity (65%) and FLT3 selectivity (FLT3/JAK1 = 8×), therefore prompting us to explore alternative approaches to circumvent the FLT3 off-target activity.

The second strategy depicted in Figure 3 relied on exploring the solvent front region by targeting the guanidine side-chain moiety of the JAK1-specific residue Arg-879 via modification of the R_2 imidazole substituent. In place of arginine, FLT3 contains an amino side-chain in Lys-614, while JAK2 has a primary carboxamide in Gln-853. It was hypothesized that the introduction of a polar functional group, such as a carboxylic acid or derivative, could potentially establish a favorable 2-point interaction with the guanidine moiety in Arg-879, while electrostatically disfavoring binding to both key off-targets, FLT3 and JAK2.

Initial efforts at replacing the benzimidazole ring as a handle to engage the JAK1 solvent front Arg-879 residue included a variety of mono- and di-substituted imidazoles (Table 5). This effort did result in several potent and JAK1 selective analogs (i.e., JAK2/JAK1 = 125× for **16**), however the diminished kinome selectivity and large cell shift (>1000-fold for **16**) ultimately led us to deprioritize further work on the acyclic imidazoles.

Interestingly, in addition to the generally poor kinome selectivity, the imidazoles often exhibited diminished JAK1 isoform selectivities compared to benzimidazole **10**, despite having the previously optimized cyclohexyl diamine moiety (see **17**, Table 5). The lack of isoform selectivity was mainly driven by a loss in the JAK1 on-target potency, as this structural change did not have a significant impact on the JAK2 binding. Calculations of the strain energies associated with adopting a JAK1 bioactive conformation suggest that imidazole **17** only pays 0.1 kcal/mol higher energy penalty to adopt the JAK1 bioactive conformation relative to benzimidazole **10**, an energy difference that is not sufficiently large to account for the diminished potency and selectivity profile.[10] One

Table 5
In vitro JAK enzyme activity and selectivity for selected imidazoles and saturated benzimidazoles

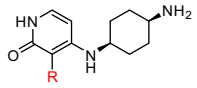

Entry	R	JAK1 (nM)	JAK2/JAK1 ratio	FLT3/JAK1 ratio	Kinome selectivity[a,b] (%)
16	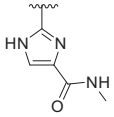	3	125	na	na
17	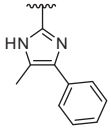	6	5	25	73
18	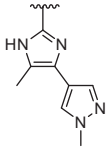	13	26	na	na
19 (R^1 = H)	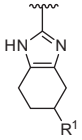	0.9	33	25	98
20 ($R^1 = CHF_2$)[c]		0.4	27	59	90
21 (R^1 = COOMe)		0.8	48	105	99
22 (R^1 = COOH)		1.3	50	158	98

[a] Percent of kinases with >100-fold selectivity against JAK1.
[b] na = not available.
[c] Racemic.

hypothesis is that, unlike with the more compact benzimidazoles, the bulkier imidazole substituent (i.e., Ph in **17**) clashes with the Glu-966 side-chain, therefore weakening the optimal RNH_2—H_2O—Glu interaction needed for JAK1 potency and selectivity (see Fig. 4).

Given the initial results and the favorable selectivity profile of the benzimidazoles, efforts were shifted away from the acyclic imidazoles and onto the more closely related saturated benzimidazoles to potentially arrive at a more optimal handle to engage the Arg-879 residue (see **19**–**22**, Table 5). The unsubstituted partially saturated benzimidazole **19** showed a comparable potency and selectivity profile to **10**, however the introduction of a polar substituent on the cyclohexyl C3 position in proximity to the guanidine moiety (i.e., carboxylic acid or ester) led to a potent

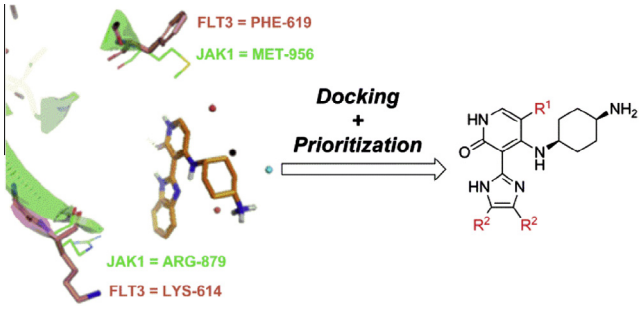

Figure 3. Two strategies to address FLT3 off-target activity based on X-ray structure of **10** (orange) in JAK1 (green) overlaid with known FLT3 crystal structure (purple; RCSB PDB code: 4XUF).

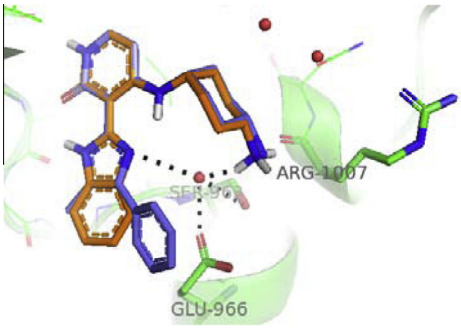

Figure 4. Docked structure of **17** (blue) in JAK1 (green) overlaid with the X-ray structure of **10** (RCSB PDB code: 5HX8).

Table 6
In vitro JAK enzyme, cell activities and off-target profile for **21**

Enzymatic IC_{50}	Cellular IC_{50}	JAK1-fold selectivity
JAK1 = 0.8 nM JAK2 = 40 nM JAK3 = 17 nM TYK2 = 7 nM	JAK1 (IL-6) = 44 nM JAK2 (EPO) = 1699 nM	NUAK1 = 14× FLT3 = 105×

JAK1 inhibitor **21** with much improved kinome selectivity of 99%. More importantly, this structural modification increased the FLT3 off-target margin to >100-fold relative to JAK1 and led to further improvement in the JAK2/JAK1 selectivity (48-fold).

Similar effects on the isoform and kinome selectivity, including the FLT3 activity, were seen with other polar groups, such as the carboxylic acid in **22**. As hypothesized in Figure 3, this effect diminished as the polar cyclohexyl substituent was replaced with other non-polar groups such as the difluoromethyl in **20** or the trifluoromethyl group (not shown). Therefore, targeting the solvent-front Arg-879 in JAK1 provided a dual benefit in optimizing both FLT3 and JAK2 off-target activities for this new class of JAK1 inhibitors. It is also worth noting that the JAK1 selectivity over JAK2 in the biochemical assays seen with **21** (48-fold) correlated well with the cell-based EPO and IL-6 pathway reporter gene assays (39-fold), as shown in Table 6.[16]

In parallel to optimizing the Arg-879 solvent-front interaction, the ribose pocket (P-loop) SAR (Fig. 1) was revisted to identify a few acyclic amines with improved kinome selectivities relative to **10** (Fig. 5). The objective with this effort was to arrive at ribose pocket substitution that would more optimally occupy the P-loop region compared to **10**, while still engaging the JAK1-specific Glu-966 residue. To achieve this dual effect, a variety of bidirectional, acyclic diamines were designed and prepared, using analog **23** as the starting point. Saturated benzimidazole propane 1,3-diamine **23** was identified as a potent and kinome selective JAK1 inhibitor that optimally occupied the P-loop region of the ribose pocket, albeit with modest JAK2/JAK1 selectivity (12-fold). Using a docking of **23** overlaid with the original crystal structure of cyclohexyl diamine **10**, several bidirectional hybrid analogs were prepared to simultaneously occupy the P-loop and engage the Glu-966 residue. This approach indeed proved successful and led to our most selective JAK1 inhibitor **24** prepared up to that point with JAK2/JAK1 and FLT3/JAK1 selectivities of 102-fold and 145-fold, respectively. Compound **24** also highlights the potential to modulate FLT3 off-target activity in the P-loop region, in addition to the solvent-front SAR. One could envision that additional JAK1 and FLT3 selectivity could be gained by engaging the Arg-879 solvent-front residue as shown in Figure 3 in conjunction with the optimized basic amine in **23**.

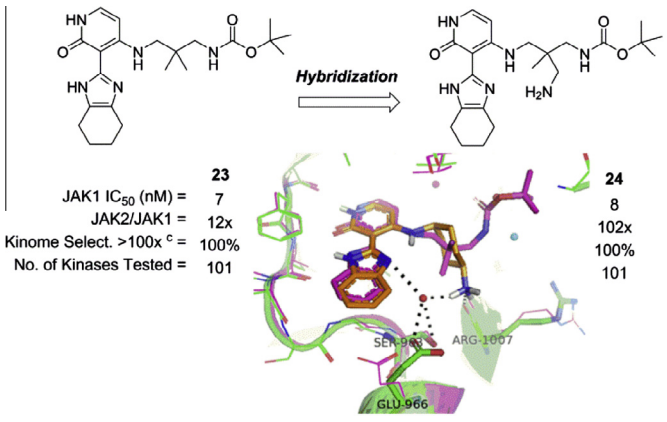

Figure 5. X-ray structure of **10** (orange) in JAK1 (green) overlaid with docking of **23** (purple) used to design hybrid **24**; [c] Kinome selectivity over non-JAK kinases.

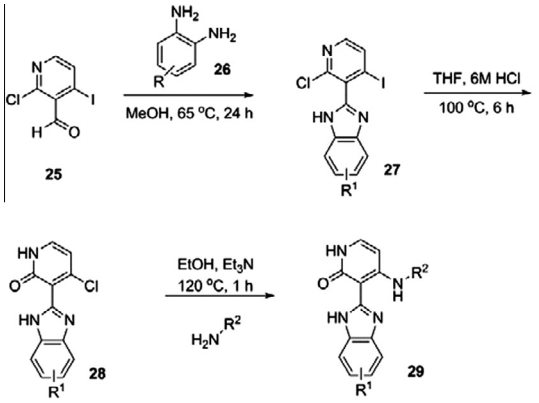

Scheme 1. General synthetic route to substituted benzimidazole pyridones.

The synthesis of the benzimidazole pyridones is described in Scheme 1.[7] Initial condensation of pyridine aldehyde **25** with the appropriately substituted diamine **26** afforded benzimidazole **27**. Hydrolysis of the 2-Cl pyridine moiety to afford the desired pyridone was accomplished under acidic conditions with concomitant replacement of the iodide with a chloride. Lastly, the ribose pocket amine was introduced under standard S_NAr conditions to afford the desired benzimidazole pyridone **29**.

The synthesis of the imidazole pyridines followed a modified synthetic approach. Condensation of an alternative starting pyridine aldehyde **30** with the appropriate dicarbonyl derivative **31** in the presence of ammonium hydroxide in MeOH at ambient temperature[17] cleanly afforded the desired imidazole pyridines **32**, which were subsequently transformed to the desired pyridones **34** as described in Schemes 1 and 2.

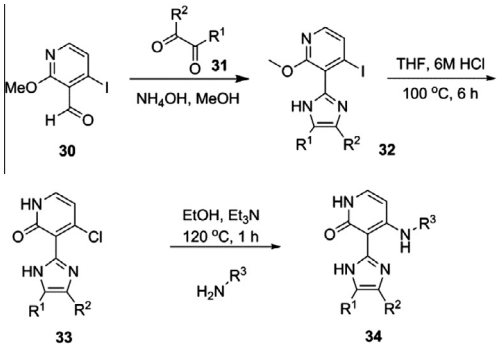

Scheme 2. General synthetic route to substituted imidazole pyridones.

In conclusion, a new series of highly JAK1 and kinome selective (benz)imidazole pyridone inhibitors has been optimized using extensive structure-based design and computational modeling. Two JAK1-specific residues, Arg-879 and Glu-966, were identified and specifically targeted to circumvent key JAK2 and FLT3 off-target activities. A bidirectional ribose pocket substitution was also identified that optimally occupied the P-loop region, while engaging the JAK1-specific Glu-966 residue. We believe that the strategies described herein can be broadly applied to other structural classes toward the design of novel JAK1 inhibitors with good selectivities over JAK2 and the rest of the kinome.

Acknowledgments

Special thanks to Andrew Haidle and Daniel McMasters for careful review of the manuscript, Bruce Adams for NMR support, as well as David Smith and Lisa Nogle for purification support.

Supplementary data

Supplementary data (the enzyme vs cell ratios) associated with this article can be found, in the online version, at http://dx.doi.org/10.1016/j.bmcl.2016.02.035.

References and notes

1. Schindler, C.; Levy, D. E.; Decker, T. *J. Biol. Chem.* **2007**, *282*, 20059.
2. (a) O'Shea, J. J. *Immunity* **1997**, *7*, 1; (b) Pesu, M.; Laurence, A.; Kishore, N.; Zwillich, S. H.; Chan, G.; O'Shea, J. J. *Immunol. Rev.* **2008**, *223*, 132; (c) Ghoreschi, K.; Laurence, A.; O'Shea, J. J. *Immunol. Rev.* **2009**, *228*, 273.
3. Tofacitinib for RA: (a) Zerbini, C. A.; Lomonte, A. B. *Expert Rev. Clin. Immunol.* **2012**, *8*, 319; Ruxolitinib for RA: (b) Mesa, R. A.; Yasothan, U.; Kirkpatrick, P. *Nat. Rev. Drug Disc.* **2012**, *11*, 103; Ruxolitinib for myelofibrosis: (c) Vaddi, K.; Sarlis, N. J.; Gupta, V. *Expert Opin. Pharmacother.* **2012**, *13*, 2397.
4. (a) Riese, R. J.; Krishnaswami, S.; Kremer, J. *Best Pract. Res. Clin. Rheumatol.* **2010**, *24*, 513; (b) Verstovsek, S.; Kantarijian, H.; Mesa, R. A.; Pardanani, A. D.; Cortes-Franco, J.; Thomas, D. A.; Estrov, Z.; Fridman, J.-S.; Bradley, E. C.; Erickson-Viitanen, S.; Vaddi, K.; Levi, R.; Tefferi, A. *N. Engl. J. Med.* **2010**, *363*, 1552; (c) Laurence, A.; Pesu, M.; Silvennoinen, O.; O'Shea, J. J. *Open Rheumatol. J.* **2012**, *6*, 232.
5. Compounds were tested in two cell-based assays for their ability to inhibit cytokine induced signaling, including (a) IL-6 stimulation related to JAK1/2-pSTAT3 pathway signaling and (b) EPO stimulation related to JAK2-pSTAT5 pathway signaling. In general, we have observed good correlation between the enzymatic JAK2/JAK1 ratio and the cell EPO/IL-6 ratio. See the Supporting information for more details.
6. (a) Brubaker, J.; Close, J.; Siu, T.; Smith, G. F.; Torres, L.; Woo, H. C.; Young, J.; Wei, Z.; Shi, F. WO 2013/041042, A1.; (b) Brubaker, J.; Childers, M. L.; Christopher, M.; Close, J.; Katz, J. D.; Jung, J.; Peterson, S.; Siliphaivanh, P.; Siu, T.; Smith, G. F.; Torres, L. E.; Woo, H. C.; Young, J. R.; Zhang, H. WO 2013/043962, A1.; (c) Zhang, H.; Siliphaivanh, P.; Siu, T.; Torres, L.; Brubaker, J.; Nagayoshi, M.; Martinez, M.; Close, J.; Childers, M.; MacCoss, R.; Young, J. R.; Dinsmore, C. J.; Jones, P.; Li, C.; Jung, J.; Pickford, F.; Deshmukh, S. V. *Abstracts of Papers*, 248th ACS National Meeting & Exposition, San Francisco, CA, United States, 2014; MEDI-372.
7. (a) Prior to our work, pyridone benzimidazoles had been described in the literature as tyrosine kinase inhibitors having anti-cancer activity. See: Wittman, M. D.; Balasubramanian, N.; Velaparthi, U.; Zimmermann, K.; Saulnier, M. G.; Liu, P.; Sang, X.; Frennesson, D.; Stoffan, K. M.; Tarrant, J. G. WO 2002/079192, A1.; (b) Velaparthi, U.; Wittman, M.; Liu, P.; Carboni, M. J.; Lee, F. Y.; Attar, R.; Balimane, P.; Clarke, W.; Sinz, M. W.; Hurlburt, W.; Patel, K.; Lorell, D.; Kim, S.; Gottardis, M.; Greer, A.; Li, A.; Saulnier, M.; Yang, Z.; Zimmermann, K.; Trainor, G.; Vyas, D. *J. Med. Chem.* **2008**, *51*, 5897.
8. Ultimately, the goal was to achieve EPO/IL-6 pathway selectivity of 15-fold or higher in the cell-based pathway reporter gene assays in order to differentiate our compounds from the currently marketed pan-selective JAK inhibitors. For a discussion on previously reported strategies to displace or engage a conserved water molecule in medicinal chemistry, see: (a) Stahl, M.; Kuhn, B.; Bissantz, C. *J. Med. Chem. (Perspective)* **2010**, *53*, 5061; (b) Dunitz, D. J. *Science* **1994**, *264*, 670.
9. For an example exploring the P-loop hypothesis toward JAK1 selectivity, see: Friedman, M.; Frank, K. E.; Aguirre, An.; Argiriadi, M. A.; Davis, H.; Edmunds, J. J.; George, D. M.; George, S. J.; Goedken, E.; Fiamengo, B.; Hyland, D.; Li, B.; Murtaza, A.; Morytko, M.; Somal, G.; Stewart, K.; Tarcsa, E.; Van Epps, S.; Voss, J.; Wang, L.; Woller, K.; Wishart, N. *Bioorg. Med. Chem. Lett.* **2015**, *25*, 4399.
10. Calculations were performed at the B3LYP/6-31+G(d) level of theory by using the G09 program in implicit solvent model (iefpcm).
11. Upon completion of this work, a similar observation was made and published by Genentech in their effort to identify a JAK1-selective inhibitor. See: Zak, M.; Hurley, A. C.; Ward, S. I.; Bergeron, P.; Barrett, K.; Balazs, M.; Blair, W. S.; Bull, R.; Chakravarty, P.; Chang, C.; Crackett, P.; Deshmukh, G.; DeVoss, J.; Dragovich, P. S.; Eigenbrot, C.; Ellwood, C.; Gaines, S.; Ghilardi, N.; Gibbons, P.; Gradl, S.; Gribling, P.; Hamman, C.; Harstad, E.; Hewitt, P.; Johnson, A.; Johnson, T.; Kenny, J. R.; Koehler, M. F. T.; Bir Kohli, P.; Labadie, S.; Lee, W. P.; Liao, J.; Liimatta, M.; Mendonca, R.; Narukulla, R.; Pulk, R.; Reeve, A.; Savage, S.; Shia, S.; Steffek, M.; Ubhayakar, S.; van Abbema, A.; Aligas, I.; Avitabile-Woo, B.; Xiao, Y.; Yang, J.; Kulagowski, J. J. *J. Med. Chem.* **2013**, *56*, 4764.
12. Functional selectivity for IL-6 signaling versus EPO signaling was performed by measuring the inhibition of EPO driven proliferation of human CD34+ hematopoietic stem cells and IL-6 driven secretion of MCP1 from human PBMCs.
13. IL-7 signaling in human and/or rat whole blood was measured by stimulating with IL-7 and measuring pSTAT5 in the CD3+ CD4+ cell subset by flow cytometry.
14. Tested at Invitrogen using SelectScreen™ Kinase Profiling (www.thermofisher.com).
15. (a) Whartenby, K. A.; Calabresi, P. A.; McCadden, E.; Nguyen, B.; Kardian, d.; Thianhong, W.; Mosse, C.; Pardoll, D. M.; Small, D. *Proc. Natl. Acad. Sci. U.S.A.* **2005**, *102*, 16741; (b) Karsunky, H.; Merad, M.; Cozzio, A.; Weissman, I. L.; Manz, M. G. *J. Exp. Med.* **2003**, *198*, 305.
16. The only measured non-JAK kinase that showed <100-fold IC_{50} activity relative to JAK1 was NUAK1. NUAK1 is a member of the AMPK (AMP-activated protein kinase) family of protein kinases that are activated by the LKB1 tumor suppressor kinase and plays an important role in regulating key biological processes, such as tumorigenesis, senescence, cell adhesion and neuronal polarity. There is some evidence suggesting that NUAK1 participates in induction of tumor survival, however, for the most part, its detailed biological functions remain unclear. See: (a) Hou, X.; Liu, J. E.; Liu, W.; Liu, C. Y.; Liu, Z. Y.; Sun, Z. Y. *Oncogene* **2011**, *30*, 2933; (b) Banerjee, S.; Buhrlage, S. J.; Huang, H. T.; Deng, X.; Zhou, W.; Wang, J.; Traynor, R.; Prescott, A. R.; Alessi, D. R.; Gray, N. S. *Biochem. J.* **2014**, *457*, 215.
17. Rodgers, J. D.; Robinson, D. J.; Arvanitis, A. G.; Maduskuie, T. P. Jr.; Shepard, S.; Storace, L.; Wang, H.; Rafalski, M.; Jalluri, R. K.; Combs, A. P.; Crawley, M. L. WO 2005/105814, A1.